

SCATTERING DOMAINS AROUND THE RECIPROCAL LATTICE POINTS OF BENZIL CRYSTAL BY PHOTOGRAPHIC PHOTOMETRY *

By R. K. SEN

DEPARTMENT OF X-RAYS AND MAGNETISM INDIAN ASSOCIATION
FOR THE CULTIVATION OF SCIENCE, CALCUTTA 32.

(Received for publication, August 29, 1952)

Plates I A-C

ABSTRACT. Equi-intensity lines around the (42.0), (22.0) and (40.2) reciprocal lattice points of benzil in the different reciprocal lattice planes have been drawn from the measurements of the intensity distribution in the different extra spots observed in the Laue photographs of benzil. The shapes of the equi-intensity surfaces have been discussed in the light of the thermal theories. The observed surfaces agree with the results of the thermal theories.

INTRODUCTION

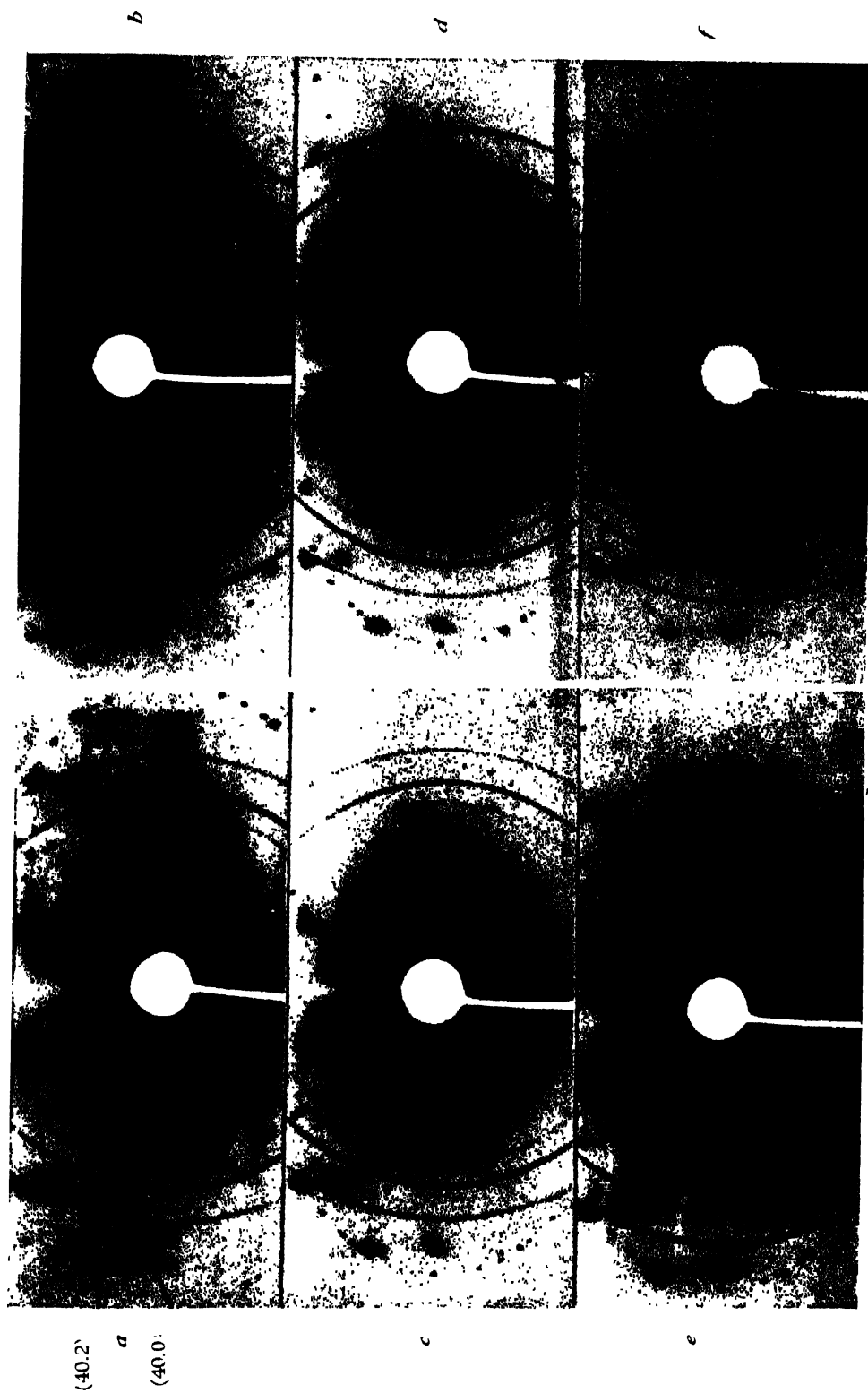
In previous communications, Lonsdale and Smith (1951), Banerjee, Sen and Khan (1945) and Sen (1947) reported a number of interesting results of the measurements of the positions of the extra spots and streaks in the Laue photographs of benzil. For a proper understanding of how far these extra spots of benzil conform to thermal diffuse-scattering it is necessary that the scattering domains around the reciprocal lattice points are mapped from a study of these extra reflections. Such mappings were first carried out by Laval (1939) who drew iso-diffusion lines or lines drawn through points having equal diffuse scattering power around the reciprocal lattice points of sylvine. Since then the scattering domains round the reciprocal lattice points of a number of crystals, mostly cubic, have been studied. Since benzil is a noncubic molecular crystal, its investigation is expected to be very interesting. For determining the intensity distributions in the extra spots, ionisation methods have been universally used by the earlier investigators. Since a photographic method has its obvious advantages such a method has been developed in the present investigation. The mapping of equi-intensity lines around the reciprocal lattice points of benzil and discussing their shapes and forms in the light of the thermal theories of the origin of the extra reflections have been aimed at in this paper.

* Communicated by Prof. K. Banerjee

EXPERIMENTS

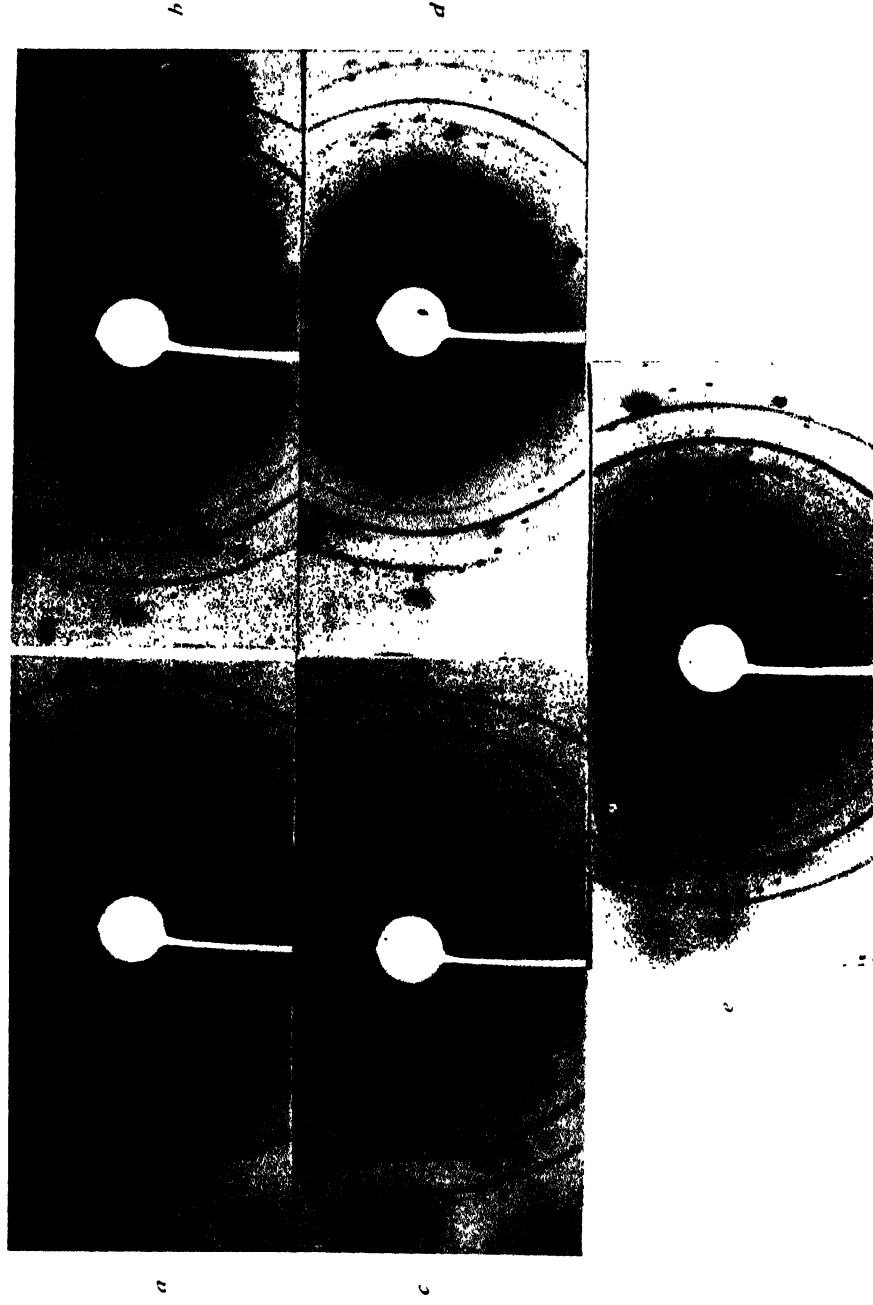
(a). A small crystal of benzil was mounted on the axis of a cylindrical camera with the $[00.1]$ axis coinciding with the axis of the camera. Unfiltered X-rays, from a North American Philips X-ray diffraction unit with copper anticathode at a voltage of 45 K. V. and 15 ma, after being collimated through a 7 cm. long slit with a cylindrical hole of about .5 mm. diameter at the narrow part, was incident on the crystal normal to the axis of the camera. Stationary crystal photographs were then taken with the X-ray beam making various angles with the $[10.0]$ axis. In each of these photographs a number of aluminium powder diffraction lines, arising out of diffraction of X-rays by a small amount of aluminium powder dusted on the crystal, were also recorded. These photographs are shown in Plates I, A-C. The whole series could not be completed with one crystal but two crystals were actually used. Same type of film and same conditions of development were used for all the photographs. The Laue photographs consisted of the usual Laue spots, corresponding to the diffraction of general X-radiations by the crystal lattice, the diffuse spots and the weak streak between these diffuse spots and comparison lines from aluminium powder. The indices of the planes giving rise to the diffuse spots were determined in the manner indicated in the previous communication by the present author (Sen, 1947).

(b) *Intensity measurements.* The intensity distribution in the diffuse spots and streaks were measured with the help of a Moll recording microphotometer. For spots lying on the equatorial line, the photographs were mounted on the carriage of the photometer in such a manner as to allow the scanning spot of light (width .02 mm. and height .5 mm) to traverse through the spots along the equatorial line when the carriage is driven by the motor of the instrument. In the same traversal two aluminium powder lines were also traversed along with the spots. For spots lying above or below the equatorial line, a traversal was given through the spots and aluminium lines parallel to the equatorial line at a height corresponding to the different layer lines to which the spots belong. Similarly for the weak streak connecting the (40.0) diffuse spot with the (40.2) diffuse spot traversals parallel to the equatorial lines at heights of 1 mm., 2 mm., 3 mm., etc. were given. The photometric curve obtained from each of these traversals gives the galvanometer deflections against distances traversed. From these curves we have to obtain intensity versus crystal orientation curves. The ordinates of the recorded photometric curves were therefore converted into intensity on an arbitrary scale by comparing them with the deflections of photometric curve of a calibration wedge obtained by the method of Robinson (1933). The abscissa of the photometric curves were converted into the corresponding angles of diffraction with the help of the observed distance between the peaks corresponding to the aluminium lines whose angles of diffractions are already known. Thus from the photometric records, the intensity (in an arbitrary



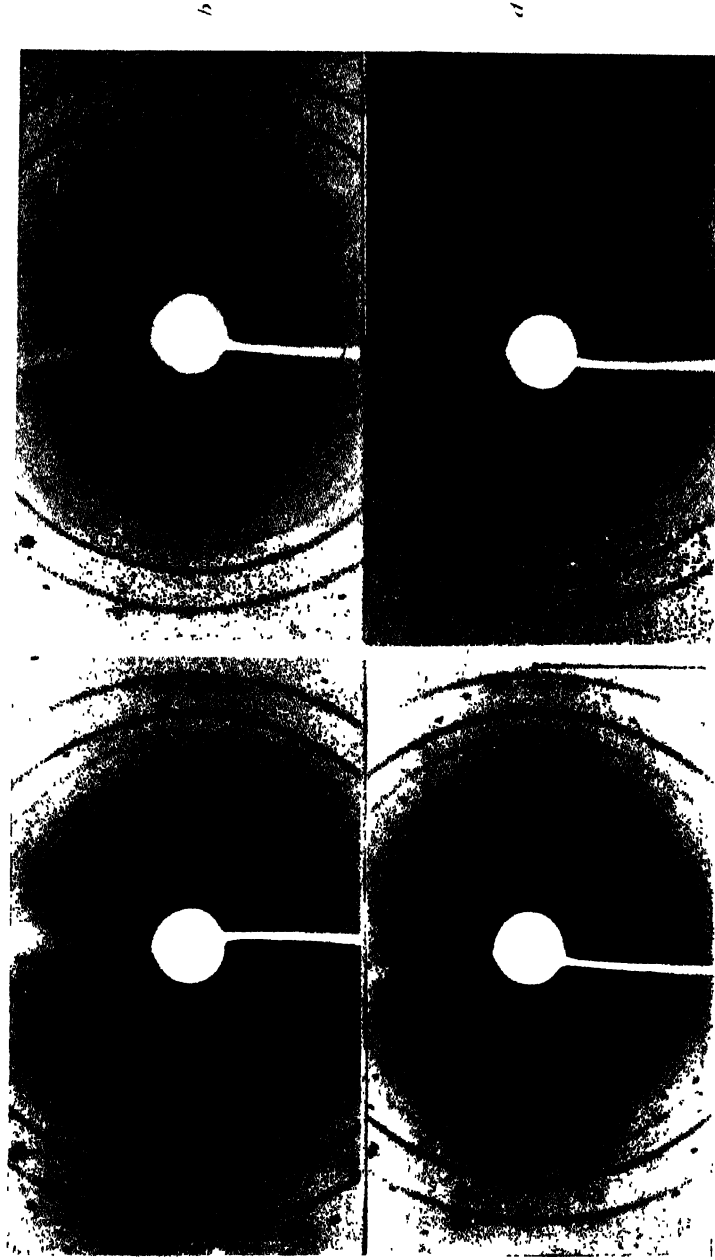
Laue photographs with incident beam making angles:

(*a*). 0°50'; (*b*). 1°24'; (*c*). 2°18'; (*d*). 3°6'; (*e*). 3°24' and (*f*). 4°6' with the [10.0] axis.
[00.1] axis vertical.



Laue photographs with incident beam making angles :

(a), $5^{\circ}10'$; (b), 6° ; (c), $6^{\circ}20'$; (d), $6^{\circ}48'$ and (e), $8^{\circ}6'$ with $[10.0]$ axis, $[00.1]$ axis vertical.



220

Laue photographs with incident beam making angles : a $20^{\circ}30'$, b $21^{\circ}6'$, c $22^{\circ}18'$ and d $22^{\circ}48'$ with $[100]$ axis. $[001]$ axis vertical.

scale)-angle of diffraction curves for the different spots and streaks observed in different photographs were computed.

In the different photographs the total intensity of the incident beam was not the same. The intensities of the diffuse scattering measured from the different photographs were brought to the same scale with the help of the ratios of the peak intensities of a particular aluminium line observed in the different photographs. The photograph taken with the incident beam making $4^{\circ}6'$ with the $[10.0]$ direction was taken as the standard and the maximum intensity in the (40.0) diffuse spot of this photograph was taken as 10. The relative intensities of the diffuse spots observed in all the photographs were then computed in the manner indicated above. For bringing to the same scale the photographs taken with different crystals, photograph in one identical position of each of the crystals was taken. The orientation in which the incident beam makes an angle of $4^{\circ}6'$ with $[10.0]$ direction was taken as the standard orientation. By comparing the intensity distribution of the same diffuse spot (40.2) in these two photographs the ratio for the conversion of the intensity of the one set to that corresponding to the other was determined. These intensity curves in arbitrary scale are shown in figures 1, 2, 3 and 4.

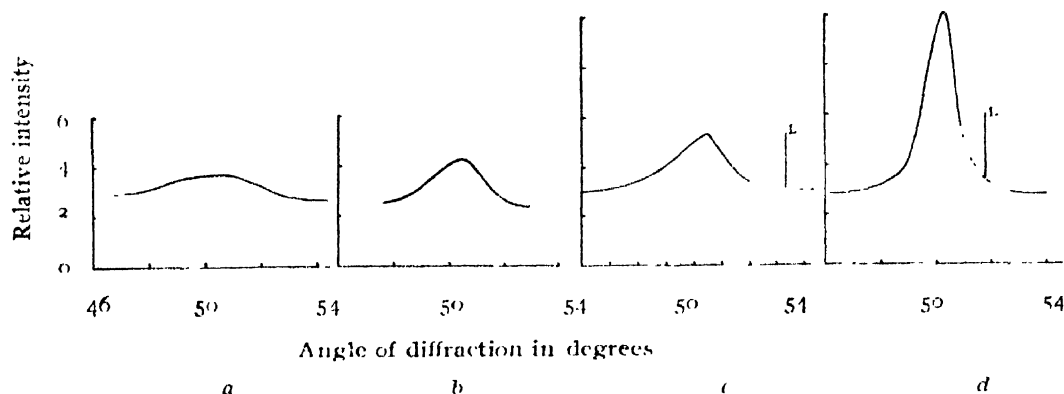


FIG. 1

Intensity distribution curve for the (40.0) extra reflection observed in the photographs taken with the incident beam making (a) $2^{\circ}18'$ ($\theta = \theta_B + 2^{\circ}36'$), (b) $3^{\circ}6'$ ($\theta = \theta_B + 1^{\circ}48'$), (c) $3^{\circ}24'$ ($\theta = \theta_B + 1^{\circ}80'$), and (d) $4^{\circ}6'$ ($\theta = \theta_B + 0^{\circ}48'$) with $[10.0]$ axis. L corresponds to the Laue reflections from the plane (40.0)

Representation on the reciprocal lattice. The reciprocal lattice of benzil (figure 5) was constructed as usual. By taking a vector OC of length $1/\lambda$, where λ is the wave-length of the radiation used ($\text{CuK}\alpha = 1.54 \text{ \AA}$), in the reciprocal lattice parallel to the incident ray such that its extremity coincides with the origin O of the reciprocal lattice and another vector CP equally of length $1/\lambda$ parallel to the diffuse ray, one finds that the vector OP

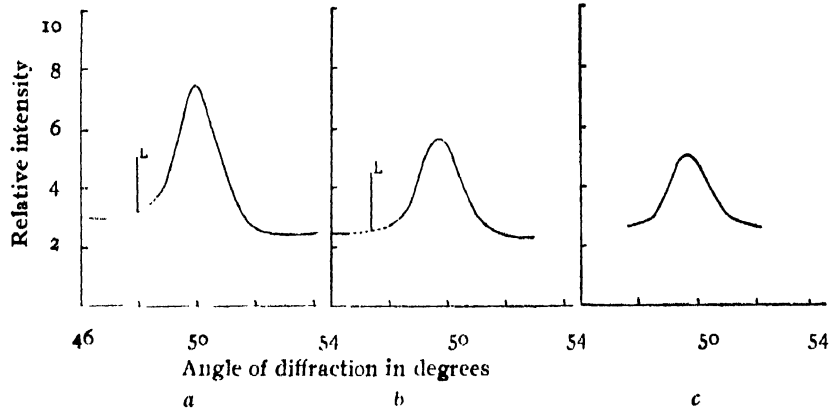


FIG. 2

Intensity distribution curve for the (40.0) extra reflection observed in the photographs taken with the incident beam making (a) 6° ($\theta_i = \theta_B - 1^\circ 0'$), (b) $6^\circ 20'$ ($\theta_i = \theta_B - 1^\circ 26'$) and (c) $6^\circ 48'$ ($\theta_i = \theta_B - 1^\circ 54'$) with $[10.0]$ axis. L represents the Laue reflection from the (40.0) plane.

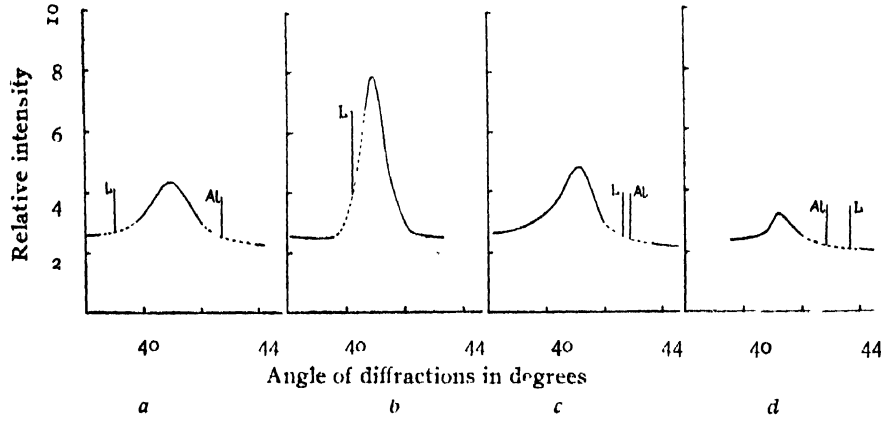


FIG. 3

Intensity distribution curve for the (22.0) extra reflection observed in the photographs taken with the incident beam making (a) $20^\circ 30'$ ($\theta_i = \theta_B + 0^\circ 56'$), (b) $21^\circ 6'$ ($\theta_i = \theta_B - 0^\circ 20'$), (c) $220^\circ 18'$ ($\theta_i = \theta_B + 0^\circ 52'$) and (d) $22^\circ 48'$ ($\theta_i = \theta_B + 1^\circ 23'$) with $[10.0]$ axis. L represents the Laue reflection from (22.0) plane. Al represents the aluminium (200) diffraction line.

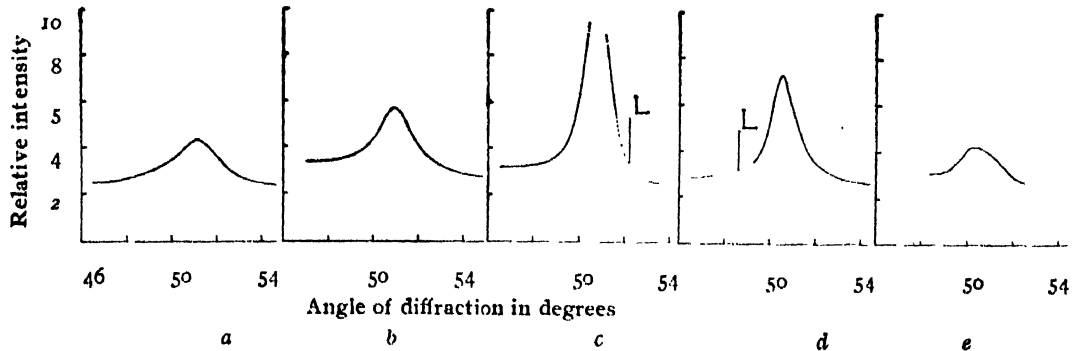


FIG. 4

Intensity distribution curve for the (40.2) extra reflection observed in the photographs with the incident beam making (a) $0^\circ 50'$, (b) $1^\circ 24'$, (c) $2^\circ 18'$, (d) $4^\circ 6'$ and (e) $5^\circ 10'$ with $[10.0]$ axis. L represents the Laue reflection from (40.2) plane.

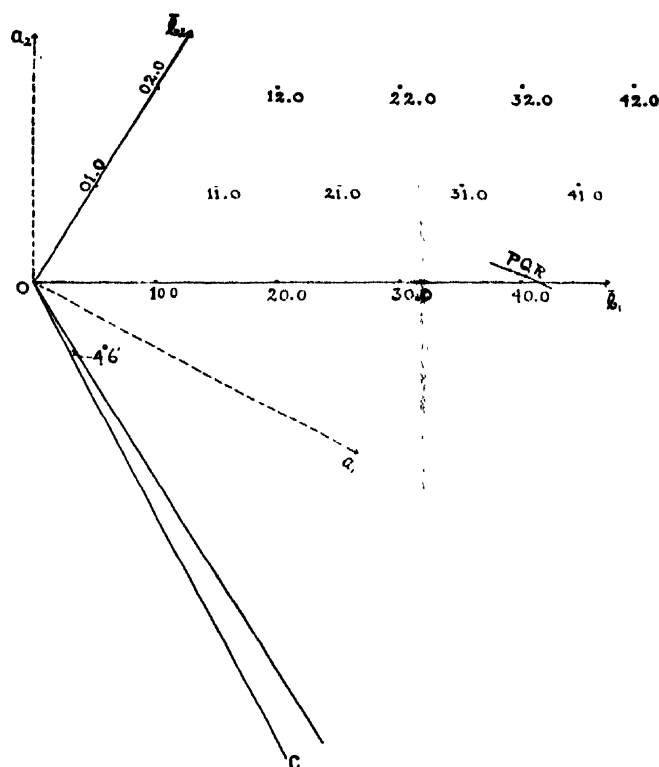


FIG. 5

A section of the reciprocal lattice of benzil normal to $[001]$ axis, which is also the b_2 reciprocal lattice axis. — reciprocal lattice axes — crystal lattice axes — P, Q, R. are the poles corresponding to angles of diffraction 49° , 50° and 51° respectively

(figure 5) is the reciprocal lattice vector responsible for the diffusion in the direction under consideration. The vector OP is called the 'vector of diffusion' and P is the 'pole of diffusion'. The selective Bragg reflection takes place when the pole of diffusion P coincides with any node M . A section of the reciprocal lattice of benzil normal to the $[00.1]$ axis and the corresponding crystal lattice is shown in figure 5. In order to draw equi-scattering surfaces (*i.e.* surfaces having equal intensity of scattering), the 'poles of diffusion', corresponding to the different points of observations in the diffuse spots, were plotted in the reciprocal lattice. From the considerations laid down above it is clear that the plotting of the 'poles of diffusion' is carried on by drawing a circle of radius $1/\lambda$ with centre C through the origin O (CO being the direction of the incident X-ray beam) and then drawing another line CP making with CO , the observed angle of diffusion corresponding to a point in the diffuse spot, when the point P , where CP meets the circle, gives the 'pole' corresponding to the point of observation considered. Some of the 'poles of diffusion', corresponding to different points in the (40.0) diffuse spot observed in the photograph with the incident beam making $4^\circ 6'$ with $[10.0]$ axis, are shown in figure 5. At the various

poles of diffusion thus plotted, the values of the relative intensities observed at the corresponding points of the relative intensity curves, were then noted. It must be noted here that relative intensity values are the values obtained by subtracting the intensity of the background from the total intensity observed at those points. Again, since the same scanning spot of light was used for the photometry of all the spots, the solid angle over which the observation is made is different for the different spots. For if ds be the area of the scanning spot of light used in photometry and ds/R be the radius of the camera used, then ds/R^2 is the solid angle over which the intensity has been measured in the case of spots lying on the equatorial line, whereas for the spots lying above or below the equatorial line this solid angle is

$$\frac{ds \cos \mu}{(R/\cos \mu)^2} = \frac{ds \cos^3 \mu}{R^2}, \text{ where } \mu \text{ is the vertical angular coordinate corresponding to the layer lines to which the spot belongs. The intensities of the spots lying on different layer lines above or below the equatorial}$$

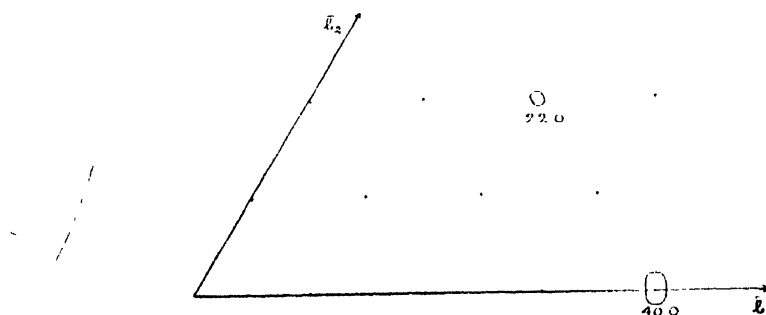


FIG. 6

Equi-intensity lines around the (40.0) and (22.0) reciprocal lattice points in the plane normal to the b_3 axis.

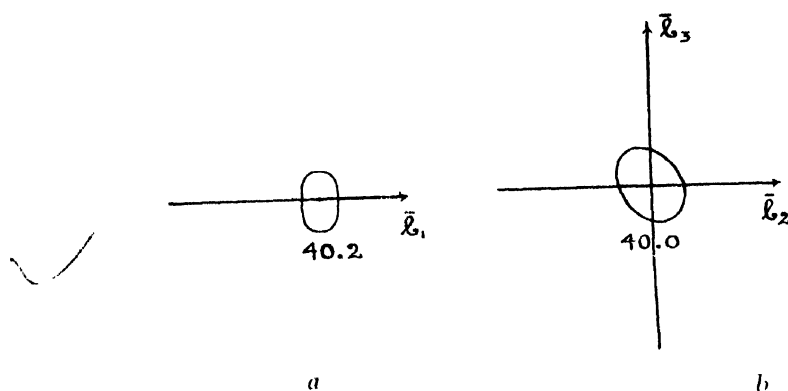


FIG. 7

(a) Equi-intensity lines around the (40.2) reciprocal lattice point in the plane perpendicular to the $[00.1]$ axis.

(b) Equi-intensity lines around (40.0) reciprocal lattice point in the $\bar{b}_2 - b_3$ plane

line were, therefore, divided by the factor $\cos^3 \mu$ in order to convert it to the intensities corresponding to the solid angle of observation used in the intensity measurement for the spots on the equatorial line. For the (40.2) spot the relative intensity values corrected in the above manner were plotted in the reciprocal lattice. Lines were then drawn through points having equal values of the relative intensities plotted. Thus equi-scattering surfaces around the different reciprocal lattice points were obtained. In figure 6 are shown the sections of the equi-scattering surfaces around the (40.0) and (22.0) reciprocal lattice points by a plane normal to the $[00.1]$ axis. A section of the scattering domain around the (40.0) reciprocal lattice point by the $\bar{b}_2 b_3$ reciprocal lattice plane is shown in figure 7.

DISCUSSION OF RESULTS

The shapes of the equi-scattering lines in the plane parallel to $b_1 b_2$ around the reciprocal lattice points (40.0), and (22.0) are more or less elliptical with the major axis along the normal to the reciprocal lattice vector. This indicates that the amplitudes of vibration due to the transverse waves are much larger than those due to the longitudinal waves. In the case of NaCl, KCl, Al also it has been observed that the thermal diffuse scattering due to transverse waves are more intense than that due to longitudinal waves. Again, the strong regions of equi-scattering lines around the reciprocal lattice points in the plane normal to $[00.1]$ axis are more or less symmetrical about the reciprocal lattice vector and its normal. The section of the equi-scattering surface around the (40.0) reciprocal lattice point by the $b_2 \bar{b}_3$ plane shows that the strong scattering regions are more or less elliptical in shape but they are not symmetrical about the b_3 axis and $\bar{b}_1 b_2$ plane. These features of the scattering domains around the reciprocal lattice points can be qualitatively explained on the thermal theories of diffuse scattering (Born, 1912-43, Zachariasen, 1940). According to these theories, the intensity of scattering I_s corresponding to a point near the reciprocal lattice points is given by the relation,

$$I_s = I_e N K T \cdot F^2 \cdot d(q) / m,$$

where
$$I_e = I_0 \left(\frac{e^2}{m_0 c^2} \right)^2 \frac{(1 + \cos^2 \phi)}{2} = \text{Thomson factor.}$$

N = no. of cells in the crystal

K = Boltzmann constant

T = Temperature

$m = \sum m_k$ where m_k is the mass of the k th atom of the cell

F = Crystal structure factor of the plane in question.

$$d(\bar{q}) = \sum D_{\alpha\beta}^{-1}(\bar{q}) q_{\beta}^{(h)}$$

$$D_{\alpha\beta}^{-1}(\bar{q}) = \text{adj}_{\alpha\beta} D(\bar{q}) / \det D(\bar{q})$$

$$\rho D(\bar{q}) = \begin{bmatrix} C_{11} & C_{66} & C_{55} & C_{65} & C_{51} & C_{16} \\ C_{66} & C_{22} & C_{44} & C_{24} & C_{46} & C_{62} \\ C_{55} & C_{44} & C_{33} & C_{43} & C_{35} & C_{54} \\ C_{65} & C_{24} & C_{43} & \frac{1}{2}(C_{23} + C_{44}) & \frac{1}{2}(C_{45} + C_{36}) & \frac{1}{2}(C_{64} + C_{15}) \\ C_{51} & C_{46} & C_{35} & \frac{1}{2}(C_{16} + C_{36}) & \frac{1}{2}(C_{31} + C_{55}) & \frac{1}{2}(C_{56} + C_{14}) \\ C_{16} & C_{62} & C_{54} & \frac{1}{2}(C_{61} + C_{25}) & \frac{1}{2}(C_{56} + C_{14}) & \frac{1}{2}(C_{12} + C_{66}) \end{bmatrix} \begin{bmatrix} \bar{q}_1^2 \\ \bar{q}_2^2 \\ \bar{q}_3^2 \\ 2\bar{q}_2\bar{q}_3 \\ 2\bar{q}_3\bar{q}_1 \\ 2\bar{q}_1\bar{q}_2 \end{bmatrix}$$

\bar{q} is the vector joining the reciprocal lattice point to the point of observation.
 $q_{\alpha}^{(h)}$, $q_{\beta}^{(h)}$ are the components of the reciprocal lattice vector along and normal to the \bar{b}_1 axis.

$C_{\alpha\beta}$ are the elastic constants. ρ is the density.

For hexagonal crystals of D_3 class to which the present crystal belongs, the determinant $\rho D(\bar{q})$ reduces to

$$\rho D(\bar{q}) = \begin{bmatrix} C_{11} & C_{66} & C_{44} & C_{14} & 0 & 0 \\ C_{66} & C_{11} & C_{44} & -C_{14} & 0 & 0 \\ C_{44} & C_{44} & C_{33} & 0 & 0 & 0 \\ C_{14} & -C_{14} & 0 & \frac{1}{2}(C_{13} + C_{44}) & 0 & 0 \\ 0 & 0 & 0 & 0 & \frac{1}{2}(C_{44} + C_{13}) & C_{14} \\ 0 & 0 & 0 & 0 & C_{14} & \frac{1}{2}(C_{12} + C_{66}) \end{bmatrix} \begin{bmatrix} \bar{q}_1^2 \\ \bar{q}_2^2 \\ \bar{q}_3^2 \\ 2\bar{q}_2\bar{q}_3 \\ 2\bar{q}_3\bar{q}_1 \\ 2\bar{q}_1\bar{q}_2 \end{bmatrix}$$

where,

$$\left. \begin{aligned} \rho D_{11}(\bar{q}) &= C_{11} \bar{q}_1^2 + C_{66} \bar{q}_2^2 + C_{44} \bar{q}_3^2 + 2C_{14} \bar{q}_2 \bar{q}_3 \\ \rho D_{22}(\bar{q}) &= C_{66} \bar{q}_1^2 + C_{11} \bar{q}_2^2 + C_{44} \bar{q}_3^2 - 2C_{14} \bar{q}_2 \bar{q}_3 \\ \rho D_{33}(\bar{q}) &= C_{44} (\bar{q}_1^2 + \bar{q}_2^2) + C_{33} \bar{q}_3^2 \\ \rho D_{23}(\bar{q}) &= C_{14} (\bar{q}_1^2 - \bar{q}_2^2) + (C_{13} + C_{44}) \bar{q}_2 \bar{q}_3 \\ \rho D_{31}(\bar{q}) &= (C_{44} + C_{13}) \bar{q}_3 \bar{q}_1 + 2C_{14} \bar{q}_1 \bar{q}_2 \\ \rho D_{12}(\bar{q}) &= 2C_{14} \bar{q}_3 \bar{q}_1 + (C_{13} + C_{66}) \bar{q}_1 \bar{q}_2 \end{aligned} \right\} \dots \quad (I)$$

For (h0.0) planes, for points lying in the plane normal to [00.1] axis and along the normal to the reciprocal lattice vector, $q_3=0$, $q_1=0$ and $q=q_2$, then equation (1) reduces to,

$$\rho D_{11}(\bar{q}) = C_{66} \bar{q}^2, \rho D_{22}(\bar{q}) = C_{11} \bar{q}^2, \rho D_{33}(\bar{q}) = C_{44} \bar{q}^2$$

$$\rho D_{23}(\bar{q}) = -C_{14} \bar{q}^2, \rho D_{31}(\bar{q}) = 0, \rho D_{12}(\bar{q}) = 0$$

$$\det D(\bar{q}) = \frac{\bar{q}^4}{\rho^3} C_{66} (C_{11} C_{44} - C_{14}^2)$$

$$\text{and } adj D_{11}(\bar{q}) = \frac{\bar{q}^4}{\rho^2} (C_{11} C_{44} - C_{14}^2)$$

$$\therefore D_{11}^{-1}(\bar{q}) = \frac{\rho}{\bar{q}^2} \cdot \frac{1}{C_{66}}$$

For the (40.0) reciprocal point, therefore,

$$d(q) = D_{11}^{-1}(\bar{q}) q^{(h)2}$$

$$\frac{\rho}{q^2} \cdot \frac{1}{C_{66}} \sigma^{(h)2}$$

where, $q^{(h)}$ is equal to the reciprocal lattice vector and q is the distance of the point of observation, lying on the normal to $q^{(h)}$, from the reciprocal lattice point. It is observed, therefore, that since q^2 is involved in the expression for the intensity, the intensity will be practically the same so long as \bar{q} remains the same in magnitude no matter whether the point of observation lies on one side or the other. It must be mentioned here, however, that the intensity will vary very slightly for the very small difference in the corresponding angles of diffraction. Similarly it can be shown that for all points lying on the plane normal to [00.1 axis] the intensity depends on \bar{q}^2 , that is to say the intensity depends on the magnitude of \bar{q} and not on its sign except for the small difference in angle of diffraction. Thus it is found that according to the thermal theories, the section of the scattering surface around (40.0) by the $\bar{b}_1\bar{b}_2$ plane will be practically symmetrical about \bar{b}_1 axis and the normal to it. This is in agreement with the observations.

Again, for points lying in the $\bar{b}_2\bar{b}_3$ plane but not falling on \bar{b}_2 or \bar{b}_3 , none of the values of q_1 , q_2 and q_3 are zero, so in this case, the expressions for $D_{11}(\bar{q})$, $D_{22}(\bar{q})$, $D_{33}(\bar{q})$ etc., will be those given by equation (1). For the $\bar{b}_2\bar{b}_3$ plane through (40.0) reciprocal lattice point, the expression for $d(\bar{q})$ is given by, $d(\bar{q}) = D_{11}^{-1}(\bar{q}) \bar{q}^{(h)2}$, since $q_2^{(h)}$ and $q_3^{(h)}$ are zero.

$$D_{11}^{-1}(\bar{q}) = \frac{D_{22}(\bar{q})D_{33}(\bar{q}) - D_{23}^2(\bar{q})}{\det D(\bar{q})}$$

$$\therefore d(q) = \frac{D_{22}(q)D_{33}(\bar{q}) - D_{23}^2(q)}{\det D(q)} \cdot q^{(h)}$$

Now, in the expression for $D_{22}(\bar{q})$ there is a term $-2C_{14}\bar{q}_2 q_3$. Hence $D_{22}(\bar{q})$ will have different values for the positive and negative values of \bar{q}_3 having the same magnitude. So $d(q)$ and consequently the intensity of scattering corresponding to points in $b_2 b_3$ plane at equal distances from the (40.0) reciprocal lattice point on the two sides of the $b_1 b_2$ plane will have different values. The scattering surface will not therefore be symmetrical about the $b_1 b_2$ plane. The present observations are therefore quite in agreement with the theory. Quantitative comparison cannot be carried on as the elastic constants are not known. However, from the above considerations it is clear that so far as the strong diffuse scatterings are concerned the intensity distribution is in general agreement with the thermal theories.

ACKNOWLEDGMENT

Thanks are due to Prof. K. Banerjee, D. Sc., F. N. I. for constant help and guidance during the progress of the work.

REFERENCES

- Banerjee, K., Sen, R. K., and Khan, Md Ferdouse, 1945, *Proc. Nat. Inst. Sci. Ind.*, **11**, 4.
 Born, M., 1942-43, *Rep. Phys. Soc. Progr. Phys.*, **9**, 294.
 Laval, J., 1939, *Bull. Soc. franc. Minér.*, **62**, 137.
 Lonsdale, K and Smith, H., 1941, *Proc. Roy. Soc. A*, **179**, 8.
 Robinson, B. W , 1933, *J. Sci Instr.*, **10**, 233.
 Sen, R. K., 1947, *Ind. J. Phys* , **21**, 285.
 Zachariasen, W. H., 1944, *Theory of X-ray diffraction in Crystals* John Wiley and Sons, Inc. New York.